Comparing the accuracy of 3D urban olive tree models detected by smartphone using LiDAR sensor, photogrammetry and NeRF: a case study of ’Ascolana Tenera’ in Italy

Stefano Chiappini[1], Mattia Balestra[1], Federico Giulioni[1], Ernesto Marcheggiani[1], Eva Savina Malinverni[2], Roberto Pierdicca[2]

[1]Department of Agricultural, Food and Environmental Sciences (D3A), Via Brecce Bianche, Ancona, 60131, Italy, IT;
[2]Department of Civil, Building Engineering and Architecture (DICEA), Via Brecce Bianche, Ancona, 60131, Italy, IT;

Keywords: Urban tree, LiDAR, smartphone, Mobile Laser Scanner, NeRF, Photogrammetry

Abstract

Rapid urban growth makes green space management crucial to improve citizens’ well-being. Urban olive trees characterize the Italian landscapes and their culture. This study explores different methodologies for urban tree assessment in this context, using an iPhone 14 Pro Max. These included: 1) its integrated Light Detection and Ranging (LiDAR) sensor using the Recon3D app, 2) its camera with Structure from Motion (SfM) techniques, and 3) its camera for generating 3D models using Neural Radiance Fields (NeRF). Additionally, a professional Mobile Laser Scanner (MLS), was used for comparison. Total height (H), canopy base height (CBH) and canopy volume (CV) measurements were extracted using both CloudCompare and allometric formulas. The main aim of this paper is to compare the 3D models of olive trees obtained from low-cost sensors with those generated from the MLS, which is a more accurate device but comes with significantly higher costs. The results, in terms of RMSE (iPhone LiDAR - H: 0.46 m, CBH: 0.12 m, CV: 15.66 m3; iPhone-SfM - H: 0.95 m, CBH: 0.19 m, CV: 25.85 m3; iPhone-NeRF - H: 1.26 m, CBH: 0.31 m, CV: 33.79 m3), bias and volume differences, reveal that the smartphone, in all the methodologies, tends to underestimate measurements as the size of the trees increases. This is due to the higher MLS range of acquisition. Despite these limitations, low-cost solutions like smartphone-based methods can be a viable alternative given their economic accessibility.

1. Introduction

In recent decades, the increase in urban population and the expansion of urban areas have had a significant impact on the quality of life of citizens. According to data from the United Nations, in 2018, 55% of the world’s population lived in urban areas, and it is projected to reach 68% by 2050 (Ritchie and Roser, 2018). While cities offer many advantages and opportunities to people, they face serious issues related to climate change and environmental pollution. Among these, but not limited to, we can list the urban heat island effect, air pollution, and the reduction of biodiversity. This increasingly relevant scenario has led local administrations to address the growing need to promote a better quality of life through the creation and maintenance of public green spaces where trees play a central role (Mensah et al., 2016; Artmann et al., 2019; Gavrilidis et al., 2022). In addition to providing significant ecosystem services, some plants also represent a symbol of cultural identity and tradition for a city. This is evident in the case of the city of Ascoli Piceno, located in central Italy, where the olive variety known as the “Ascolana Tenera” plays a crucial role in local agriculture. Its presence is widespread throughout the Ascoli territory, including the historic center of the city, a testament to the deep bond that the community has with this cultivar. Derived from the homonymous variety of the “Olea europaea” species, the “Ascolana Tenera” represents a genuine excellence in the agricultural sector of the Marche region, to the extent of receiving the prestigious DOP (Protected Designation of Origin) recognition and being designated as “Oliva Ascolana del Piceno”. Its importance has prompted local authorities to protect it even within the context of urban greenery, through a census aimed at collecting the main dendrometric parameters (tree height (H), canopy base height (CBH) and canopy volume (CV)), that are essential for conducting accurate inventory and for managing these resources optimally. The determination of the CV represents a particularly challenging task. The traditional methods used so far involve intensive work for the multiple manual measurements that need to be carried out, which also have limitations due to intra- and inter-individual variability, making the measurements subjective and not reproducible. To address this issue, especially in recent years, the rapid advancement of three-dimensional (3D) digitization and reconstruction, besides artificial intelligence (AI) technologies presents new opportunities in the field of trees’ monitoring and conservation. These cutting-edge technologies facilitate the implementation of sophisticated approaches in forestry, facilitating precise data collection and the automatic generation of models (Huang et al., 2024). This method allows for obtaining detailed information on tree characteristics and its dendrometric parameters (Wallace et al., 2016). To obtain 3D data on trees, among terrestrial platforms, we find terrestrial laser scanning (TLS), mobile laser scanning (MLS), and ground-based photogrammetry. TLS ensures the highest geometric precision of data among all sensors and platforms, while MLS collects data efficiently, albeit with slightly lower precision compared to TLS. On the other hand, ground-based photogrammetry processes images captured by various cameras and is commonly used and easy to operate (Balestra et al., 2024). This approach, when applied to 3D tree reconstruction, forestry inventory and vegetation modeling, proves to be automated and effective in terms of representation (Iglhaut et al., 2019). However, its accuracy is strongly influenced by the complexity of the morphological branching structures of trees and the shading of internal branches caused by leaves, as well as the technical characteristics of the camera sensor.

Novel techniques capable of precisely reconstructing the entire 3D tree canopies from images are based on deep learning approaches. Neural Radiance Fields (NeRF) (Mildenhall et al., 2021) is a neural network used to synthesize novel views of complex 3D scenes by optimizing an underlying continuous

This contribution has been peer-reviewed. The double-blind peer-review was conducted on the basis of the full paper.
https://doi.org/10.5194/isprs-annals-X-3-2024-61-2024 | © Author(s) 2024. CC BY 4.0 License.

volumetric scene function based on an initial set of sparse views (Tancik et al., 2023) . MLPs (Multi-Layer Perceptrons) are trained to generate 3D objects from two-dimensional images. A 5D vector function is taken as input: the MLP takes a 5D coordinate, composed of spatial coordinates within the scene $(\mathbf{x}, \mathbf{y}, \mathbf{z})$ and two angles, azimuthal and polar, which define the viewing direction (θ, ϕ). It outputs a volumetric density, denoted as σ, and an RGB color, dependent on the viewing direction (Croce et al., 2024). The resolution-invariant nature of NeRF's implicit representation allows much more detailed and nuanced modeling, free from the constraints of resolution-dependent approaches. This capability holds significant promise in tree research, as NeRF's capacity to capture intricate details could lead to groundbreaking discoveries in plant structures, positioning it as a pivotal tool in the progression of contemporary agricultural and forestry studies (Arshad et al., 2024).

In our work, we explored two different devices: a professional MLS (*KAARTA Stencil-2*) and the low-cost iPhone 14 Pro Max, utilizing both its LiDAR and camera sensors. Initially, we employed LiDAR technology from both the iPhone (referred to as iPhone LiDAR) and the MLS (referred to as *KAARTA*) to generate the 3D models. For the iPhone, we used the Recon-3D app (Recon 3D Website, n.d.), designed for iOS mobile devices. For the second approach has been employed photogrammetry principles, specifically using the Structure from Motion (SfM) method (Schonberger and Frahm, 2016) to generate 3D point clouds from video frames captured with the iPhone camera sensors. Agisoft Metashape software was employed for this purpose. Finally, we utilized NeRF, leveraging deep learning capabilities to synthesize seamless 3D scenes captured by the iPhone camera sensors. This study highlights the potential of geomatics applications in surveying urban olive trees, integral to the Italian traditional landscape in urban and peri-urban contexts. The primary objective of this study is to compare the results of acquisitions made with the iPhone, specifically using LiDAR, SfM and NeRF, against those obtained with the KAARTA Stencil-2. Additionally, we aim to compare SfM and NeRF using the same input data. Our intention is to evaluate the applicability of the low-cost RGB camera and LiDAR mounted on a smartphone for detection and point cloud generation for metric data extraction. We highlight the strengths and limitations of using these devices in terms of generating volumetric 3D scenes that produce novel views and the resolution of the resulting point clouds. Our results, in terms of RMSE, bias, and volume differences, reveal that the smartphone tends to underestimate measurements as the size of the trees increases. By doing so, we hope to contribute to the ongoing development and refinement of this innovative approach to 3D tree reconstruction.

In Section 2, the state of the art related to 3D modeling of urban trees using various technologies is presented. In Section 3, the materials and methods used in our study are described, including details about the devices (KAARTA-Stencil 2 and iPhone 14 Pro Max) and data acquisition techniques (LiDAR, photogrammetry, and NeRF). Section 4 presents the results of the visualization and measurement of the dendrometric parameters of olive trees. In Section 5, we discuss the results obtained from the different acquisition methodologies.

2. Related works

In the past years, tree structural and geometrical parameters, as CV and CBH, were typically obtained through manual measurements of canopy height and width. However, due to the slow and costly nature of this methodology, alternative methods have been increasingly employed over the last decade (Chiappini et al., 2022b). Various technologies can be employed for the geometric characterisation of crops, including digital photographs (Balestra et al., 2023), ultrasound-based systems (Zaman and Schumann, 2005), stereoscopic images (Rovira-Más et al., 2005), high-resolution radar images (Bongers, 2001), light sensors (Castillo-Ruiz et al., 2016), and laser sensors (Sola-Guirado et al., 2018). It is important to emphasise that not all the technologies mentioned earlier have proven equally effective in accurately depicting the 3D structure of trees, primarily due to real-world field conditions. Within these options, LiDAR and stereoscopic vision systems stand out as likely the most promising methods for acquiring 3D images and maps of plants and canopies (Rosell and Sanz, 2012). One of the widely utilised approaches for quantifying biophysical parameters of olive trees involves the application of stereoscopic vision techniques, specifically utilising the SfM method (Eltner and Sofia, 2020). This method entails employing RGB cameras, with or without an infrared filter, enabling the reconstruction of 3D images. The benefit of these technologies resides in their easy-to-use and reliable application, combined with their cost efficiency (Roma and Catania, 2022). In the work of Caruso et al. (2019), the authors study the capability of UAVs equipped with RGB-NIR cameras to estimate the leaf area index, H, canopy diameter, and CV of irrigated or rain-fed olive trees. In particular, they propose a methodology for estimating the CV of trees based on the processing of Digital Terrain Model (DTM) and Digital Surface Model (DSM) generated through the SfM technique, data obtained from a low-cost RGB camera. In addition, the study conducted by Zarco-Tejada et al. (2014) showed that the use of consumer-grade cameras on unmanned aerial platforms can ensure precision similar to that achieved with LiDAR systems. The use of a low-cost camera allowed for the acquisition of high-resolution images, which were employed to create orthomosaics and Digital Surface Models (DSM) through automated 3D reconstruction techniques. Using statistical parameters, this approach proved to be economically advantageous compared to the use of expensive and complex LiDAR systems, commonly utilised in agriculture and environmental applications. In the same context, Anifantis et al. (2019) demonstrated that precise assessments of tree canopy structure and morphology can be achieved through the utilisation of an affordable drone with a simple RGB camera. To achieve this, they acquired images with a camera mounted on a DJI SPARK, which is a low-cost UAV. This sensor enabled the creation of an orthomosaic, and reconstruction of a DSM using the SfM technique. Subsequently, GIS analysis was employed to calculate the height and diameter of the canopy. A DSM represents a digital representation of a topographic surface, including both the ground and objects on it, and can be utilised to gather information about tree heights. On the other hand, a DTM only represents the ground height, excluding the height of objects present. Similar results have been obtained in the work proposed by Díaz-Varela et al. (2015), within the context of olive tree breeding programs, applicable to both fragmented and continuous canopy cropping systems.

Many studies have employed LiDAR technology, facilitating the precise, impartial, and swift determination of morphological parameters. An example is the paper of Sola-Guirado et al. (2018) that uses 2D LiDAR sensors, able to obtain a point cloud corresponding to a section of the object of interest. They successfully acquired dynamic measurements suitable for quan-

tifying the canopy in diverse agricultural activities. As evidenced in the study by Escolà et al. (2017), where the LiDAR sensor was employed, the authors achieved a remarkably strong correlation with manual estimation. Moreover, they succeeded in discerning the behaviour of sunlight within the canopy by the coefficient of determination. Possessing detailed spatial information on canopy geometry (height, width, and volume) and canopy structure (light penetration, leafiness, and porosity) can result in improved decisions for orchard management. Overall, compared to the methods discussed earlier, this technology offers the advantage of achieving substantially higher resolution levels, albeit at the expense of being more expensive.

Finally, it is necessary to refer to works that are based on deep learning approaches (Mescheder et al., 2019), which have experienced rapid progress in various fields, including computer graphics and 3D reconstruction. NeRF stands out as a notable recent development in this realm, with applications that come from virtual reality (Deng et al., 2022) to architectural reconstruction (Tancik et al., 2022). The objective, given a set of calibrated images as input, is to produce a volumetric 3D scene capable of rendering new viewpoints. In the work of Arshad et al. (2024), to evaluate the performance of NeRF method, the authors employed different methods of NeRFs to reconstruct plants in 3D across diverse environments, spanning from indoor settings (single and multiple corn plant indoor) to outdoor environment (multiple corn plants in a field with other plants. They examined three scenarios of increasing complexity and compared the results with the point cloud obtained using LiDAR as ground truth data. The experimental results highlighted the effectiveness and accuracy of NeRFs in challenging environments. In another recent work (Huang et al., 2024), the authors study underscores NeRF’s potential for tree reconstruction by applying the NeRF technique to create detailed 3D models of individual trees using images from various cameras. These models were compared with those generated by photogrammetric reconstruction and laser scanning methods. The findings indicate that NeRF excels in tree reconstruction, boasting higher accuracy and efficiency, especially in canopy areas, with fewer input images. However, NeRF-generated point clouds often suffer from noise and low resolution. Moreover, photogrammetric methods yield more accurate structural parameters.

3. Materials and methods

3.1 Detection using KAARTA-Stencil 2

This study was conducted in the city of Ascoli Piceno (in the Marche Region), which features a typically Mediterranean climate characterized by hot and dry summers (26°C) and mild winters (7°C). The average annual precipitation of around 700 mm delineates an ideal climatic environment for this variety of olive tree. The study area of our research is located near the “Istituto Tecnico Agrario, Celso Ulpiani” where, in the adjacent green area, there are olive trees of the “Ascolana Tenera” variety. As part of our research, the data acquisition campaign was conducted on April 29, 2023. The dendrometric parameters of each olive tree, derived from the point cloud obtained through the MLS (Table 1, Figure 2a), have been used as reference metrics to evaluate the accuracy of the detection obtained through the ”low-cost” device and its different sensors (Figure 1).

LiDAR	Laser units	Velodyne VPL-16
	Acquisition mode	Time of flight
	Range	1 m [min] + 100 m [max]
	Field of view	$360° \times 30°$
	Accuracy	$\pm$30 mm
	Speed	300000 points/sec
Features Tracker	Resolution	640×360
	Frequency	50 Hz
	Image colour	black and white
Computer	CPU	Intel NUC 7i7 Quad Core
	Operating system	Ubuntu Linux
	Memory	1 TeraByte
	Ports	2 HDMI, 4 USB, Rj-45 Gigabit Ethernet
	Output data	.ply, .las
IMU	Type	MEMS
	Degrees of freedom	X,Y,Z, roll, pitch, yaw
Physical characteristics	Dimensions	$162mm \times 111mm \times 141mm$
	Weight	1.73 Kg

Table 1. The main technical specifications of KAARTA-Stencil 2

3.2 LiDAR iPhone 14 Pro Max integrated with Recon-3D APP

The low-cost device used is an iPhone 14 Pro Max: a model released in September 2022. Technological advancement has introduced inexpensive and miniaturized LiDAR sensors to the market, such as those implemented by Apple in the mobile devices since 2020. While primarily designed for augmented reality applications, these sensors can also be used as measurement tools (Murtiyoso et al., 2021; Spreafico et al., 2021). They operate in both indoor and outdoor environments, with measurement capabilities up to 4.9 m in distance (Spreafico et al., 2021). The camera plays a crucial role in this context, contributing to the coloring of points in the cloud and the creation of the entire point structure (Murtiyoso et al., 2021; Spreafico et al., 2021).

The data were acquired using the ”Recon-3D” application (version 1.3.2), which provides a raw point cloud of the urban olive tree with real colors captured by the camera (Figure 2b). Recon-3D leverages Apple’s LiDAR sensor, combining it with photogrammetry to generate 3D point cloud data in the .e57 format. The Recon-3D iOS app is developed using the EveryPoint engine, created by EveryPoint, a company based in Redmond (USA). During the scanning process, the application collects LiDAR data, video at a resolution of 1920 × 1440 pixels, and the IMU information related to the device’s position and orientation. The distances measured by the LiDAR sensor are used to generate a depth map, which is then combined with frames from the recorded video Kottner et al. (2023). Upon launching, it prompts the user to name the new survey project. Subsequently, a screen appears with various parameters, among which the most significant is the “scan density”, adjustable in a range from 1 mm to 30 mm. This parameter is of fundamental importance as it determines how many measurement points will be acquired within a specific area or volume. In other words, the ”scan density” defines how detailed and accurate the representation of the scanned object or environment will be. A higher scan density implies the acquisition of a greater number of points, thereby contributing to obtaining a more precise representation of the details and features of the surface or scanned object but increasing the processing time needed. During the data acquisition phase, we opted for a “scan density” configuration of 5 mm. This decision was driven by the goal of striking a balanced compromise between acquisition accuracy and data pro-

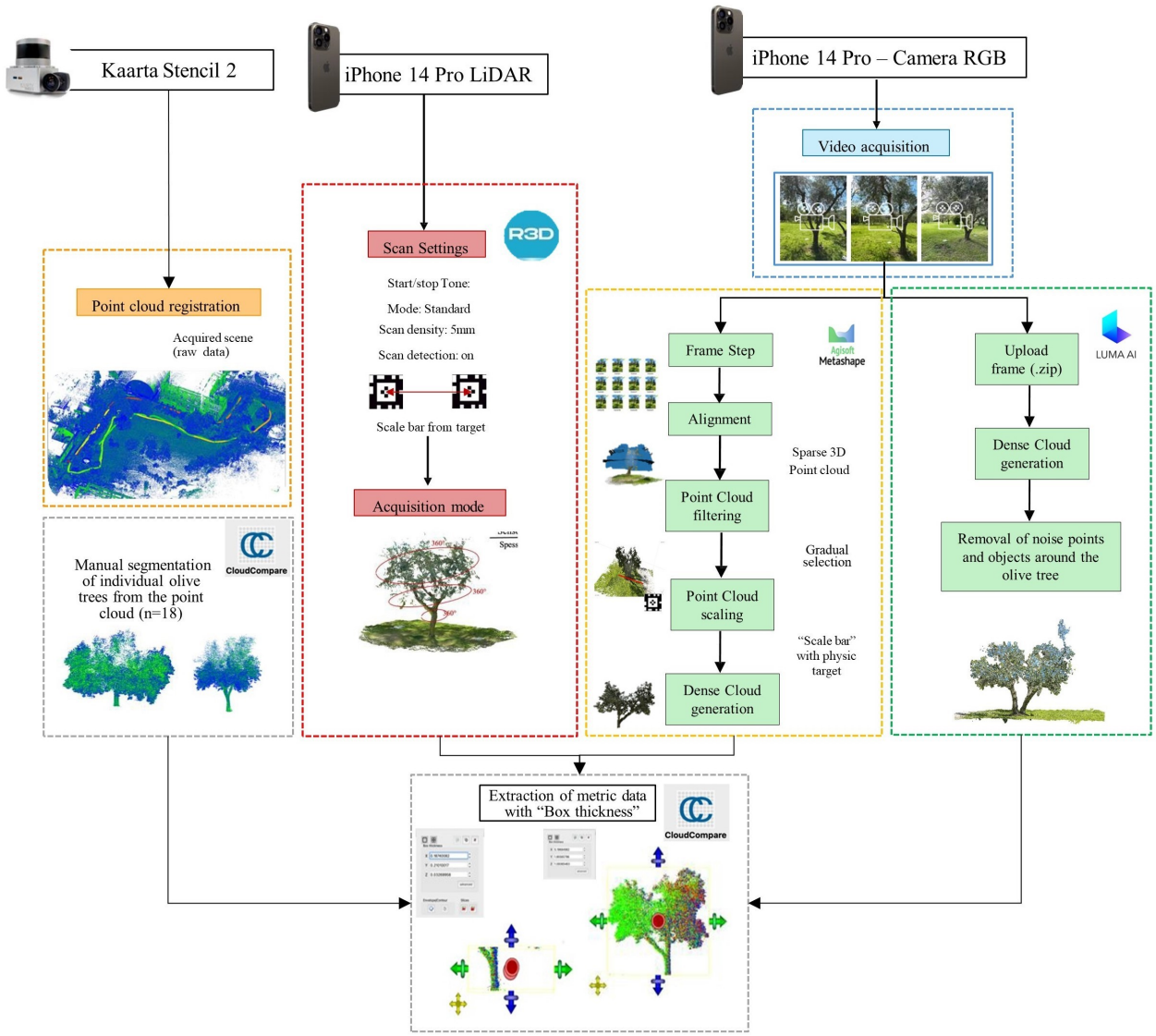

Figure 1. Workflow for validation analysis that compares the MLS results from KAARTA Stencil 2 with those obtained from the iPhone 14 Pro, both through LiDAR data captured with the Recon-3D app and the frames extracted from the RGB camera video, initially processed in Agisoft Metashape and then using NeRF models via the Luma.ai app iOS.

cessing speed. Another crucial parameter is “target detection”. The application itself provides printable targets to be strategically placed within the scanning scene. Additionally, the scaling process can be further optimised and expedited by manually entering the distance between the two targets positioned in the scanned scene. This distance, between the centres of the targets, can be entered into the application, enhancing the scaling of the point cloud and increasing both precision and processing speed. The process proceeds with exporting the raw point cloud in the .e57 format, a format easily accessible and viewable in most commercial software designed for point cloud processing (Figure 2b). Specifically, the Cloud Compare software was utilised for executing all the mentioned measurements.

3.3 iPhone 14 Pro Max: terrestrial photogrammetry application and NeRF

During this research, in addition to leveraging the capabilities of the LiDAR sensor on the iPhone 14 Pro Max, we also utilized the device’s camera system. Specifically, videos (1920 x 1440 pixels) of each olive tree were recorded at 60 fps during the use of Recon-3D. These low-resolution frames served as the basis for creating 3D models of the olive trees through both a photogrammetry process using Agisoft Metashape software and the NeRF application (Figure 1). The extraction of frames from the video was carried out using Metashape software, which, starting from version 1.3, supports this functionality. A relevant parameter is the “frame step”, which allows defining the sampling intervals during the frame extraction. To strike a balance between data quality and process manageability, a “frame step” of 15 was chosen, with the number of frames varying based on the duration of the video, typically between 3-5 minutes maximum for each tree. Before proceeding with the alignment, an additional assessment of the frame quality was conducted using the “Estimate quality image” function, which assigns a value ranging from 0 to 1 to estimate the image quality. During the alignment phase, Metashape identifies and matches homologous points in each frame, automatically obtaining the camera calibration parameters and the shooting position for each frame, generating the point cloud (Figure 2c). At the end of this phase, the model is scaled by manually enter-

ing the measurement of the distance between the targets, using the settings data collected in the Recon-3D app during the survey of each individual olive tree. Nowadays there are several tools that use NeRF models (Mildenhall et al., 2021), including the Instant NGP application, developed by Müller et al. (2022) for NVIDIA. This application has a codebase built on CUDA and Python 3.9, while camera pose estimation is performed via COLMAP. Another interesting option is NeRFstudio (Tancik et al., 2023), a more recent Python framework that allows the creation, training, and end-to-end testing of NeRFs. However, for our case study, we chose to use the cloud-based software by LumaLabs (Luma.ai, accessed on 1 March 2024), named “Luma.AI”. Neural rendering and mesh generation of the object are obtained using either a folder containing the images extracted from the video or directly uploading the video of the object detected, both at high resolution. The total time for neural rendering and mesh generation depends on the duration of the video or the number of frames uploaded. At the end of the process, it is possible to export the point cloud in .ply or .obj format and scale it using the distances between the targets.(Figure 2d).

3.4 Visualisation and measurement of point

After acquiring the point clouds using the various surveying tools, the subsequent phase entailed extracting metric data pertaining to the dendrometric parameters of each olive tree. To perform the measurements, we utilized the free software CloudCompare (Girardeau-Montaut, 2021). CloudCompare is a free and open-source software platform specialized in the analysis and manipulation of three-dimensional point clouds. The “Box Thickness” tool facilitates the creation of a virtual box for precise measurement of dimensions along the x, y, and z axes. The dendrometric parameters measured include total height (H), canopy base height (CBH), and canopy diameter (CD). CBH is calculated from the difference between the total height and the distance from the first branch of the canopy to the ground; CD is derived as the average of two diameters measured in the North-South and East-West directions. The volume of the olive canopy (CV, in m^3) was calculated using the paraboloid model, based on the canopy diameter (CD, in meters) and canopy base height (CBH, in meters), as described in equation 1 (Chiappini et al., 2022a; Estornell et al., 2017; Velázquez-Martí et al., 2012).

$$CV = \frac{1}{2}\frac{\pi CD^2 CBH}{4} \tag{1}$$

3.5 Data analysis

Following the completion of all required measurements and the analysis of the obtained results, a comparative analysis of the detection approaches was undertaken to assess the accuracy of the measurements. For this purpose, both absolute (equation 2) and percentage (equation 4) RMSE (Root Mean Square Error) and bias (equation 3) statistics were employed, referring to the dendrometric parameters of total height (H), canopy base height (CBH), and parabolic canopy volume (CV). The calculation of these metrics provides an objective and quantitative method to assess the degree of discrepancy between the values obtained from the different detection instruments (iPhone-SfM, iPhone-LiDAR and iPhone-NeRF) and the reference values, represented by measurements made with the KAARTA Stencil 2.

$$RMSE = \sqrt{\frac{1}{n}\sum_{i=1}^{n}(x_i - \hat{x}_i)^2} \tag{2}$$

$$bias = \frac{1}{n}\sum_{i=1}^{n}(x_i - \hat{x}_i) \tag{3}$$

$$RMSE\% = \frac{RMSE}{\bar{y}} \times 100 \tag{4}$$

The parameter x_i represents the values measured by iPhone-SfM/LiDAR/NeRF, $\hat{x}_i$ represents the value observed with the KAARTA Stencil 2, n is the total number of analyzed trees, and $\bar{y}$ represents the mean of the reference values detected via KAARTA-Stencil 2.

4. Experimental results

The accuracy performance of the iPhone 14 Pro Max LiDAR (Table 2) reveals a tendency to underestimate the measurements related to the H of the olive tree, with a bias of -0.26 m. Furthermore, the LiDAR exhibits a RMSE of 0.46 m and a relative RMSE% of 9.05%. However, concerning measurements of the CBH, the statistical metrics demonstrate excellent accuracy performance, with a bias of 0.04 m, an RMSE of 0.12 m, and a relative RMSE% of 11.06%. Particularly interesting is the analysis of the CV, as it encompasses multiple submeasurements and is therefore particularly representative. In this context, the iPhone 14 Pro Max LiDAR has shown a consistent tendency to underestimate the CV, with a bias of -9.65 m^3, an RMSE of 15.66 m^3, and a relative RMSE% of 40.23%. Regarding the accuracy observed in the measurements of the ground-based photogrammetry application of the iPhone 14 Pro Max (Table 3), slightly better measurements were found regarding the CBH, with a relative bias of 0 m, an RMSE of 0.19, and an RMSE% of 16.67%. However, regarding the measurements of this method concerning total height and volume, worse performances were observed compared to LiDAR. Specifically, concerning CV measurements, the bias is higher (-17.23 m^3), with an RMSE of 25.85 (RMSE% 66.4%), showing an even worse tendency to underestimate the reference measurements. The same applies to H measurements, where the bias stands at -0.73 and the RMSE at 0.95 (RMSE% 18.56%). Regarding the accuracy of the iPhone-NeRF method (Table 4), we achieved the worst measurements regarding the CBH, with a relative bias of -0.12 m, an RMSE of 0.31, and an RMSE% of 28.48%. However, regarding the measurements of this method concerning H and CV, worse performances were observed compared to iPhone-LiDAR. Concerning CV measurements, the bias is higher (-21.15 m^3), with an RMSE of 33.79 (RMSE% 84.87%), showing an even worse tendency to underestimate the reference measurements. The same applies to H measurements, where the bias stands at -0.94 and the RMSE at 1.26 (RMSE% 24.68%). As it is possible to read in table 5 and as it is possible to observe in figure 3 and 4, the measurements errors of both CV and H increase as the size of the canopy and the height of the tree increase.

5. Discussions and conclusions

The purpose of this study is to provide accurate and truthful data that can serve as a solid basis for comparing ”low-cost” sur-

(a) (b) (c) (d)

Figure 2. 3D model results of one olive tree from: (a) KAARTA Stencil 2; (b) Recon-3D app on iPhone 14; (c) Agisoft Software; (d) NeRF model obtained using the Luma.AI platform

KAARTA vs iPhone LiDAR			
	H (m)	CBH (m)	CV (m^3)
bias	-0.26	0.04	-9.65
RMSE	0.46	0.12	15.66
RMSE%	9.05	11.06	40.23

Table 2. Comparison of accuracy between KAARTA Stencil 2 and iPhone 14 Pro Max LiDAR

KAARTA vs iPhone-SfM			
	H (m)	CBH (m)	CV (m^3)
bias	-0.73	0	-17.23
RMSE	0.95	0.19	25.85
RMSE%	18.56	16.67	66.40

Table 3. Comparison of accuracy between KAARTA Stencil 2 and iPhone 14 Pro Max-SfM

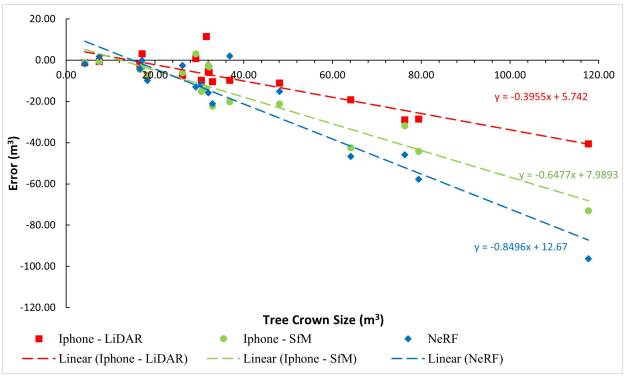

Figure 3. Volume error (m^3) related to the absolute crown size

KAARTA vs iPhone-NeRF			
	H (m)	CBH (m)	CV (m^3)
bias	-0.94	-0.12	-21.15
RMSE	1.26	0.31	33.79
RMSE%	24.68	28.48	84.87

Table 4. Comparison of accuracy between KAARTA Stencil 2 and iPhone 14 Pro Max-NeRF

Tree-ID	iPhone LiDAR		iPhone-SfM		iPhone-NeRF	
	Error (m^3)	(%)	Error (m^3)	(%)	Error (m^3)	(%)
Olive_1	-2.36	-14.20	-4.44	-26.76	-4.14	-24.92
Olive_2	-7.47	-40.81	-7.43	-40.57	-9.91	-54.10
Olive_3	-5.96	-18.53	-3.22	-10.01	NA	NA
Olive_4	-11.06	-23.00	-21.21	-44.11	-15.10	-31.40
Olive_5	3.10	18.12	-3.37	-19.73	-0.19	-1.12
Olive_6	11.48	36.30	-14.07	-44.51	NA	NA
Olive_7	-28.89	-37.87	-31.78	-41.66	-45.88	-60.14
Olive_8	-9.71	-31.86	-15.17	-49.77	-11.78	-38.65
Olive_9	-10.49	-31.79	-22.32	-67.68	-21.06	-63.84
Olive_10	-1.23	-29.55	-1.05	-25.16	-1.81	-43.42
Olive_11	-5.58	-17.44	-2.55	-7.95	-15.88	-49.61
Olive_12	-0.65	-8.76	-0.71	-9.55	1.69	22.70
Olive_13	-7.57	-28.91	-6.09	-23.27	-2.59	-9.87
Olive_14	-19.26	-30.04	-42.49	-66.27	-46.62	-72.70
Olive_15	-40.56	-34.48	-72.98	-62.04	-96.35	-81.91
Olive_16	-9.80	-26.58	-20.18	-54.72	1.99	5.39
Olive_17	0.77	2.65	3.17	10.86	-13.01	-44.58
Olive_18	-28.48	-35.86	-44.16	-55.60	-57.78	-72.75
Average	-9.65	-19.59	-17.23	-35.47	-21.15	-38.81
Dev. std	12.33	19.89	19.27	21.98	26.35	29.46

Table 5. Volume error with respect to the MLS method

veying techniques to professional sensors used to create point clouds of olive trees located in urban contexts. During this research, we conducted a detailed analysis of the main dendrometric parameters, including H, CBH, and CV. These parameters were evaluated on a total of 54 point clouds, belonging to 18 Ascolana Tenera olive trees. The instrumentation used includes both professional-grade sensors, such as the KAARTA Stencil 2, and more cost-effective solutions, such as the iPhone 14 Pro Max equipped with a LiDAR camera. In the case of the iPhone, dual sensing was adopted during acquisition, utilizing both the LiDAR actived throught the Recon-3D application and the photographic component for video acquisition as a basis for the photogrammetric process conducted with Metashape software and the NeRF model on the Luma.ai platform. Once the point clouds were obtained, the extraction of the parameters of interest was carried out within CloudCompare. From the results reported in Figures 3 and 4, concerning the calculated statistical metrics, a tendency towards satisfactory results only in measurements related to the CBH emerges in both acquisition methodologies. However, regarding the measurements of the other two parameters (H and CV), a tendency towards underestimation compared to the reference measurements obtained through the MLS is observed in both acquisition methodologies, indicating limitations especially in CV acquisition. It is important to emphasize how the larger dimensions of the olive tree to be acquired tend to significantly influence the measure-

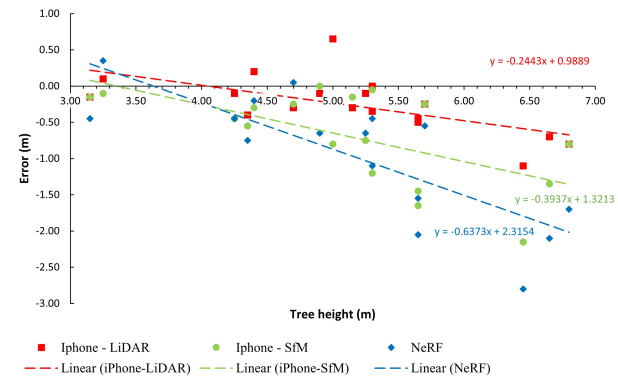

Figure 4. Total height error (m) related to the absolute tree height size

ments taken by the iPhone. In detail, the analysis of the graph relating to volume measurements highlights not only the previously mentioned tendency but also provides further significant details. Indeed, a linear relationship of increasing acquisition error with increasing canopy size of the olive tree is observed, with a more pronounced negative slope in the iPhone-SfM and iPhone-NeRF methodology. The point clouds obtained from individual trees using the iPhone, both LiDAR, SfM and NeRF, have a significant number of noisy points that require manual filtering, which could cause an incorrect interpretation by the user. Similar problems, in the field of forest inventory, have also been addressed by Huang et al. (2024), who obtained, unlike the case presented in the research, better results from NeRF as the ground data were integrated with drone images, allowing the tree to be detected in its whole entirety. A similar situation occurs in height measurements, as highlighted in Figure 4. Once again, the iPhone LiDAR shows a trend line with a lower slope compared to the iPhone-SfM and iPhone-NeRF models, indicating a relative ability to contain error as the height of the olive tree increases. Given the iPhone’s tendency to show an increase in error with increasing canopy size, we suggest improving data acquisition by using a telescopic pole. This pole can extend the iPhone’s reach to the most apical points of the canopy, providing more detailed information. The use of an extendable pole is particularly advantageous in urban settings, where drone flights can be limited by nearby buildings and the complexity of the spatial configuration, as well as by flight restrictions imposed by the national civil aviation authority.

We will further explore the full potential of this process by applying it to olive trees of different varieties and managed with various pruning techniques. Our aim is not only to understand the strengths and limitations of the iPhone’s RGB camera and LiDAR but also to reduce noise in the generated point clouds and improve the final accuracy of the required metric data. Future studies will involve recording videos in higher resolution so that the frames applied by the NeRF can recreate a smoother scene and ensure greater efficiency. In doing so, we hope to contribute to the continuous development and improvement of this low-cost approach.

6. Acknowledgements

This research is supported by the European Union - Next Generation EU through the Project of National Interest (PRIN) ”GeoIntelligence for improved air quality monitoring and analysis (GeoAIr)” 202258ACSL - PE10 at the Ministry of Higher Education and Research (MUR).

References

Anifantis, A. S., Camposeo, S., Vivaldi, G. A., Santoro, F., Pascuzzi, S., 2019. Comparison of UAV photogrammetry and 3D modeling techniques with other currently used methods for estimation of the tree row volume of a super-high-density olive orchard. *Agriculture*, 9(11), 233.

Arshad, M. A., Jubery, T., Afful, J., Jignasu, A., Balu, A., Ganapathysubramanian, B., Sarkar, S., Krishnamurthy, A., 2024. Evaluating NeRFs for 3D Plant Geometry Reconstruction in Field Conditions. *arXiv preprint arXiv:2402.10344*.

Artmann, M., Inostroza, L., Fan, P., 2019. Urban sprawl, compact urban development and green cities. How much do we know, how much do we agree? *Ecological indicators*, 96, 3–9.

Balestra, M., Choudhury, M. A. M., Pierdicca, R., Chiappini, S., Marcheggiani, E., 2024. UAV-Spherical Data Fusion Approach to Estimate Individual Tree Carbon Stock for Urban Green Planning and Management. *Remote Sensing*, 16(12), 2110.

Balestra, M., Tonelli, E., Vitali, A., Urbinati, C., Frontoni, E., Pierdicca, R., 2023. Geomatic data fusion for 3D tree modeling: The case study of monumental chestnut trees. *Remote Sensing*, 15(8), 2197.

Bongers, F., 2001. Methods to assess tropical rain forest canopy structure: an overview. *Tropical Forest Canopies: Ecology and Management: Proceedings of ESF Conference, Oxford University, 12–16 December 1998*, Springer, 263–277.

Caruso, G., Zarco-Tejada, P. J., González-Dugo, V., Moriondo, M., Tozzini, L., Palai, G., Rallo, G., Hornero, A., Primicerio, J., Gucci, R., 2019. High-resolution imagery acquired from an unmanned platform to estimate biophysical and geometrical parameters of olive trees under different irrigation regimes. *PLoS One*, 14(1), e0210804.

Castillo-Ruiz, F. J., Castro-Garcia, S., Blanco-Roldan, G. L., Sola-Guirado, R. R., Gil-Ribes, J. A., 2016. Olive crown porosity measurement based on radiation transmittance: an assessment of pruning effect. *Sensors*, 16(5), 723.

Chiappini, S., Giorgi, V., Neri, D., Galli, A., Marcheggiani, E., Savina Malinverni, E., Pierdicca, R., Balestra, M., 2022a. Innovation in olive-growing by proximal sensing lidar for tree volume estimation. *2022 IEEE Workshop on Metrology for Agriculture and Forestry (MetroAgriFor)*, 213–217.

Chiappini, S., Pierdicca, R., Malandra, F., Tonelli, E., Malinverni, E. S., Urbinati, C., Vitali, A., 2022b. Comparing Mobile Laser Scanner and manual measurements for dendrometric variables estimation in a black pine (Pinus nigra Arn.) plantation. *Computers and Electronics in Agriculture*, 198, 107069.

Croce, V., Forleo, G., Billi, D., Bevilacqua, M., Piemonte, A., Caroti, G., 2024. Neural Radiance Fields (Nerf) For Multi-Scale 3D Modeling Of Cultural Heritage Artifacts. *The International Archives of the Photogrammetry, Remote Sensing and Spatial Information Sciences*, 48, 165–171.

Deng, N., He, Z., Ye, J., Duinkharjav, B., Chakravarthula, P., Yang, X., Sun, Q., 2022. Fov-nerf: Foveated neural radiance fields for virtual reality. *IEEE Transactions on Visualization and Computer Graphics*, 28(11), 3854–3864.

Díaz-Varela, R. A., De la Rosa, R., León, L., Zarco-Tejada, P. J., 2015. High-resolution airborne UAV imagery to assess olive tree crown parameters using 3D photo reconstruction: application in breeding trials. *Remote Sensing*, 7(4), 4213–4232.

Eltner, A., Sofia, G., 2020. Structure from motion photogrammetric technique. *Developments in Earth surface processes*, 23, Elsevier, 1–24.

Escolà, A., Martínez-Casasnovas, J. A., Rufat, J., Arnó, J., Arbonés, A., Sebé, F., Pascual, M., Gregorio, E., Rosell-Polo, J. R., 2017. Mobile terrestrial laser scanner applications in precision fruticulture/horticulture and tools to extract information from canopy point clouds. *Precision Agriculture*, 18, 111–132.

Estornell, J., Velázquez-Martí, A., Fernández-Sarría, A., López-Cortés, I., Martí-Gavilá, J., Salazar, D., 2017. Estimación de parámetros de estructura de nogales utilizando láser escáner terrestre. *Revista de Teledetección*, 67–76.

Gavrilidis, A. A., Popa, A.-M., Onose, D. A., Gradinaru, S. R., 2022. Planning small for winning big: Small urban green space distribution patterns in an expanding city. *Urban Forestry & Urban Greening*, 78, 127787.

Girardeau-Montaut, D., 2021. Cloudcompare (version 2.13.1). Accessed on December 2023.

Huang, H., Tian, G., Chen, C., 2024. Evaluating the point cloud of individual trees generated from images based on Neural Radiance fields (NeRF) method. *Remote Sensing*, 16(6), 967.

Iglhaut, J., Cabo, C., Puliti, S., Piermattei, L., O’Connor, J., Rosette, J., 2019. Structure from motion photogrammetry in forestry: A review. *Current Forestry Reports*, 5, 155–168.

Kottner, S., Thali, M. J., Gascho, D., 2023. Using the iPhone’s LiDAR technology to capture 3D forensic data at crime and crash scenes. *Forensic Imaging*, 32, 200535.

Luma.ai, accessed on 1 March 2024.

Mensah, C. A., Andres, L., Perera, U., Roji, A., 2016. Enhancing quality of life through the lens of green spaces: A systematic review approach. *International Journal of Wellbeing*, 6(1).

Mescheder, L., Oechsle, M., Niemeyer, M., Nowozin, S., Geiger, A., 2019. Occupancy networks: Learning 3d reconstruction in function space. *Proceedings of the IEEE/CVF conference on computer vision and pattern recognition*, 4460–4470.

Mildenhall, B., Srinivasan, P. P., Tancik, M., Barron, J. T., Ramamoorthi, R., Ng, R., 2021. Nerf: Representing scenes as neural radiance fields for view synthesis. *Communications of the ACM*, 65(1), 99–106.

Müller, T., Evans, A., Schied, C., Keller, A., 2022. Instant neural graphics primitives with a multiresolution hash encoding. *ACM transactions on graphics (TOG)*, 41(4), 1–15.

Murtiyoso, A., Grussenmeyer, P., Landes, T., Macher, H., 2021. First assessments into the use of commercial-grade solid state lidar for low cost heritage documentation. *XXIV ISPRS Congress (2021 edition), 5-9 juillet 2021, Nice (en ligne)*, 43.

Recon 3D Website, n.d. `https://www.recon-3d.com/`. Accessed on March 2023.

Ritchie, H., Roser, M., 2018. Urbanization. *Our world in data*.

Roma, E., Catania, P., 2022. Precision Oliviculture: Research Topics, Challenges, and Opportunities—A Review. *Remote Sensing*, 14(7), 1668.

Rosell, J., Sanz, R., 2012. A review of methods and applications of the geometric characterization of tree crops in agricultural activities. *Computers and electronics in agriculture*, 81, 124–141.

Rovira-Más, F., Zhang, Q., Reid, J., 2005. Creation of three-dimensional crop maps based on aerial stereoimages. *Biosystems engineering*, 90(3), 251–259.

Schonberger, J. L., Frahm, J.-M., 2016. Structure-from-motion revisited. *Proceedings of the IEEE conference on computer vision and pattern recognition*, 4104–4113.

Sola-Guirado, R. R., Bayano-Tejero, S., Rodríguez-Lizana, A., Gil-Ribes, J. A., Miranda-Fuentes, A., 2018. Assessment of the accuracy of a multi-beam LED scanner sensor for measuring olive canopies. *Sensors*, 18(12), 4406.

Spreafico, A., Chiabrando, F., Teppati Losè, L., Giulio Tonolo, F., 2021. The ipad pro built-in lidar sensor: 3d rapid mapping tests and quality assessment. *The International Archives of the Photogrammetry, Remote Sensing and Spatial Information Sciences*, 43, 63–69.

Tancik, M., Casser, V., Yan, X., Pradhan, S., Mildenhall, B., Srinivasan, P. P., Barron, J. T., Kretzschmar, H., 2022. Block-nerf: Scalable large scene neural view synthesis. *Proceedings of the IEEE/CVF Conference on Computer Vision and Pattern Recognition*, 8248–8258.

Tancik, M., Weber, E., Ng, E., Li, R., Yi, B., Wang, T., Kristoffersen, A., Austin, J., Salahi, K., Ahuja, A. et al., 2023. Nerfstudio: A modular framework for neural radiance field development. *ACM SIGGRAPH 2023 Conference Proceedings*, 1–12.

Velázquez-Martí, B., Estornell, J., López-Cortés, I., Martí-Gavilá, J., 2012. Calculation of biomass volume of citrus trees from an adapted dendrometry. *Biosystems Engineering*, 112(4), 285–292.

Wallace, L., Lucieer, A., Malenovskỳ, Z., Turner, D., Vopěnka, P., 2016. Assessment of forest structure using two UAV techniques: A comparison of airborne laser scanning and structure from motion (SfM) point clouds. *Forests*, 7(3), 62.

Zaman, Q.-u., Schumann, A. W., 2005. Performance of an ultrasonic tree volume measurement system in commercial citrus groves. *Precision Agriculture*, 6, 467–480.

Zarco-Tejada, P. J., Diaz-Varela, R., Angileri, V., Loudjani, P., 2014. Tree height quantification using very high resolution imagery acquired from an unmanned aerial vehicle (UAV) and automatic 3D photo-reconstruction methods. *European journal of agronomy*, 55, 89–99.